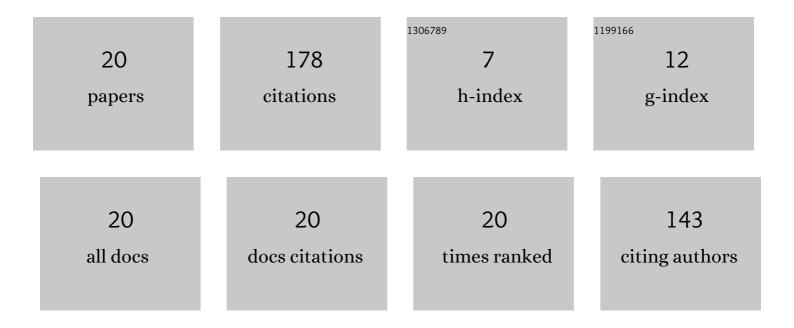
## Hongwei Wang

List of Publications by Year in descending order

Source: https://exaly.com/author-pdf/2253866/publications.pdf Version: 2024-02-01



#	Article	IF	CITATIONS
1	Source parameters, path attenuation and site effects from strong-motion recordings of the Wenchuan aftershocks (2008–2013) using a non-parametric generalized inversion technique. Geophysical Journal International, 2018, 212, 872-890.	1.0	39
2	Breakdown of Earthquake Self‧imilar Scaling and Source Rupture Directivity in the 2016–2017 Central Italy Seismic Sequence. Journal of Geophysical Research: Solid Earth, 2019, 124, 3898-3917.	1.4	23
3	Singleâ€Station Standard Deviation Using Strongâ€Motion Data from Sichuan Region, China. Bulletin of the Seismological Society of America, 2018, 108, 2237-2247.	1.1	16
4	Strongâ€Motion Observations of the 2017 MsÂ7.0 Jiuzhaigou Earthquake: Comparison with the 2013 MsÂ7.0 Lushan Earthquake. Seismological Research Letters, 2018, 89, 1354-1365.	0.8	15
5	Imprint of Rupture Directivity From Ground Motions of the 24 August 2016 <i>M</i> <sub><i>w</i></sub> 6.2 Central Italy Earthquake. Tectonics, 2017, 36, 3178-3191.	1.3	11
6	Source Characteristics, Site Effects, and Path Attenuation from Spectral Analysis of Strongâ€Motion Recordings in the 2016 KaikÅura Earthquake Sequence. Bulletin of the Seismological Society of America, 2018, 108, 1757-1773.	1.1	10
7	Attenuation and Basin Amplification Revealed by the Dense Ground Motions of the 12 July 2020 MsÂ5.1 Tangshan, China, Earthquake. Seismological Research Letters, 2021, 92, 2109-2121.	0.8	9
8	Rupture Directivity from Strong-Motion Recordings of the 2013 Lushan Aftershocks. Bulletin of the Seismological Society of America, 2015, 105, 3068-3082.	1.1	8
9	Characteristics of strong motions and damage implications of M S6.5 Ludian earthquake on August 3, 2014. Earthquake Science, 2015, 28, 17-24.	0.4	8
10	Observations on Regional Variability in Ground-Motion Amplitude from Six Mw ~ 6.0 Earthquakes of the North–South Seismic Zone in China. Pure and Applied Geophysics, 2020, 177, 247-264.	0.8	7
11	Insights on nonlinear soil behavior and its variation with time at strong-motion stations during the Mw7.8 KaikÅura, New Zealand earthquake. Soil Dynamics and Earthquake Engineering, 2020, 136, 106215.	1.9	7
12	Simulating Groundâ€Motion Directivity Using Stochastic Empirical Green's Function Method. Bulletin of the Seismological Society of America, 2017, 107, 359-371.	1.1	6
13	Probabilistic Tsunami Hazard Assessment for the Southeast Coast of China: Consideration of Both Regional and Local Potential Sources. Pure and Applied Geophysics, 2021, 178, 5061.	0.8	4
14	Seismic Wave Attenuation Characteristics from the Ground Motion Spectral Analysis around the Kanto Basin. Buildings, 2022, 12, 318.	1.4	3
15	Source Characteristics and Path Attenuation for the Yangbi, China Seismic Sequence in 2021. Pure and Applied Geophysics, 2022, 179, 2721-2733.	0.8	3
16	Investigating the Contribution of Stress Drop to Ground-Motion Variability by Simulations Using the Stochastic Empirical Green's Function Method. Pure and Applied Geophysics, 2019, 176, 4415-4430.	0.8	2
17	Earthquake Source Characteristics and S-Wave Propagation Attenuation in the Junction of the Northwest Tarim Basin and Kepingtage Fold-and-Thrust Zone. Frontiers in Earth Science, 2020, 8, .	0.8	2
18	Integrating Effects of Source-Dependent Factors on Sediment-Depth Scaling of Additional Site Amplification to Ground-Motion Prediction Equation. Bulletin of the Seismological Society of America. 0	1.1	2

#	Article	IF	CITATIONS
19	Aftershock ground motion characteristics during the 2012 Varzaghan–Ahar doublet events, northwest of Iran. Natural Hazards, 0, , 1.	1.6	2
20	Ground-motion simulation for the <i>M</i> <sub>W</sub> 6.1 Ludian earthquake on 3 August 2014 using the stochastic finite-fault method. Earthquake Science, 2019, 32, 101-114.	0.4	1